A micro snake-like robot for small pipe inspection

Shuichi Wakimoto
Okayama University

Jun Nakajima
Okayama University

Masanori Tanaka
Okayama University

Takefumi Kanda
Okayama University

Koichi Suzumori
Okayama University

A Micro Snake-like Robot for Small Pipe Inspection

Shuichi WAKIMOTO, Jun NAKAJIMA, Masanori TAKATA
Takefumi KANDA and Koichi SUZUMORI

Department of Systems Engineering, Okayama University
3-1-1 Tsushima-naka, Okayama 700-8530, Japan

Abstract:

The goal of this research is development of a micro robot which can negotiate pipes whose diameter varies widely. The robot mechanism is based on "Snaking Drive".

First, in section 1 to 4, basic characteristics of the snaking drive are discussed: the principle of the snaking drive is shown, theoretical fundamental formulas are derived, and the motions of the robot are simulated.

Second, in section 5, a micro robot was designed, fabricated and tested. And fundamental experiments of the robot are shown.

Third, in section 6, two application experiments are shown: one is a stabilization of camera image, and the other is a robot steering at branches.

The robot moved in pipes whose diameter varies between 18mm to 100mm with the maximum speed of 36mm/s. And the robot could negotiate T-branches and L-bends of pipes.

1.Introduction

In recent years, many industrial accidents owing to pipe troubles have occurred. However, most of pipes are under the ground or in complex and narrow spaces, so inspections in pipes are difficult work. Therefore development of practical inspection robot negotiating small pipes is required.

Although various pipe inspection robots have been developed [1-3], almost no robot can negotiate pipes of changing diameters. Because pipe diameter often changes, it is important for robot to adapt to pipe diameter.

This research aims at development of a micro robot, which can negotiate pipes whose diameter varies widely (1 to 3 inches).

2.Driving Principle

Several snake-like robots have been developed [4-5], and shown high potential. The authors have developed a robot negotiating in-pipe by a new snake-like locomotion using FMA (Flexible Microactuator)[6] and using a link mechanism driven by motors [7].

This research applies the snake-like locomotion to the robot configured by a miniature link mechanism and micro DC motors. This locomotion is named "snaking drive". Figure 1 shows a configuration and a driving sequence of this drive mechanism. The robot shown Fig.1 consists of 7 links and 6 rotational joints driven by sine wave signals with small phase differences between adjoining joints, and the robot moves in direction of the delayed phase link.

Target value of joint position is expressed as the following equation;

$$R(i) = A\sin\left\{\omega t - 2\pi\frac{(i-1)}{\lambda}\right\} \qquad (1)$$

where i represents the identify number of the joint, numbered from the rear to the front of the robot, A is the amplitude of bending angle, ω is the angular frequency, t is time and λ is the number of links shaping one wave, named wave length. In this research, 4-links wave length motion and 6-links wave length motion were used.

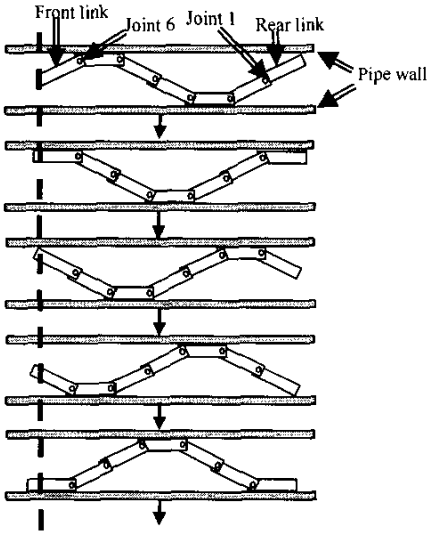

Fig.1 Driving principle of snaking drive

2003 INTERNATIONAL SYMPOSIUM ON
MICROMECHATRONICS AND HUMAN SCIENCE
0-7803-8165-3/03/$17.00 ©2003 IEEE.

Figure 1 shows an example of driving sequence by 6-links wave length (phase difference between adjoining joints is $\pi/3$). The robot moves from right side to left side using the friction between the robot and the pipe wall.

The robot can adapt to pipe diameter by changing A and selecting the wave length.

3.Theoretical characteristics

A feature of the robot is to adapt to changing pipe diameter, so it is necessary to obtain the pipe diameter to which the robot can adapt. In this section, theoretical diameter is discussed. And on the basis of it, the traveling velocity of the robot is discussed.

3.1 Theoretical adapting diameter of the robot

Theoretical diameter can be obtained as a function of the amplitude of the bending angle A geometrically. Figure 2 shows an example of static state of the robot driven by 6-links wave length.

Figure 2 leads the following equations;

$$\begin{aligned} &\theta_1 = \theta_4 = 0 \\ &\theta_2 = \theta_3 = -\theta_5 = -\theta_6 \\ &d = \left|2L\sin(\theta_2)\right| \\ &D = d + r \end{aligned} \qquad (2)$$

where D, L, d, and r represent the pipe inner diameter, the length of one link, the amplitude of the robot without diameter of the link and diameter of the link, respectively. θ_i represents the bending angle of the i-th joints, which is decided by A.

Similarly, Fig.3, which shows 4-links wave length, leads the following equations;

$$\begin{aligned} &\theta_1 = \theta_2 = -\theta_3 = -\theta_4 = \theta_5 = \theta_6 \\ &d = \left|L\cos(\theta_1)\right| \\ &D = d + r \end{aligned} \qquad (3)$$

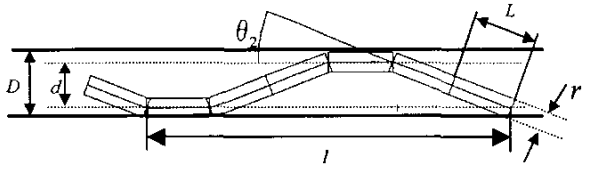

Fig.2 Geometrically state of the robot (6-links wave length motion)

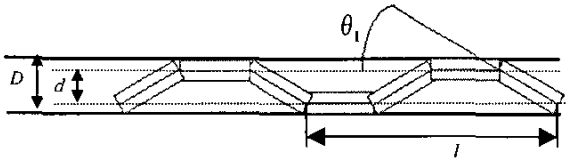

Fig.3 Geometrically state of the robot (4-links wave length motion)

The results are shown in Fig.4. These results are derived using the size of designed robot in section 5 (L = 59 mm, r = 14 mm).

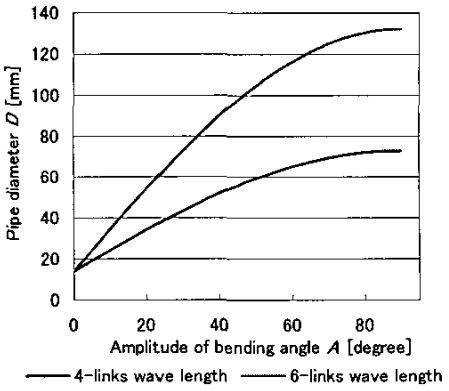

Fig.4 Theoretical adapting pipe diameter of the robot

3.2 Theoretical traveling velocity

Theoretical velocity is also obtained geometrically as a function of the amplitude of the bending angle A. Therefore, the velocity is represented as a function of the pipe diameter D from section 3.1. Define the velocity parameter of v as the traveling distance caused during a snaking cycle, or $2\pi/\omega$. Hence the parameter v has the dimension of mm/cycle.

Figure 2 leads the following equation;

$$l = 2L(1 + 2\cos(\theta_2)), \qquad (4)$$

where l is the length of a sine wave of the robot measured in the axial direction.

And v is obtained by the following equation;

$$v = 6L - l. \qquad (5)$$

Similarly, Fig.3 leads the following equations;

$$\begin{aligned} &l = 2L(1 + \cos(\theta_1)) \\ &v = 4L - l. \end{aligned} \qquad (6)$$

The results of the theoretical velocity are shown in Fig.5. The 4-links wave length motion is advantageous in small pipe diameter. And as the

pipe diameter is larger, the 6-links wave length motion is more advantageous.

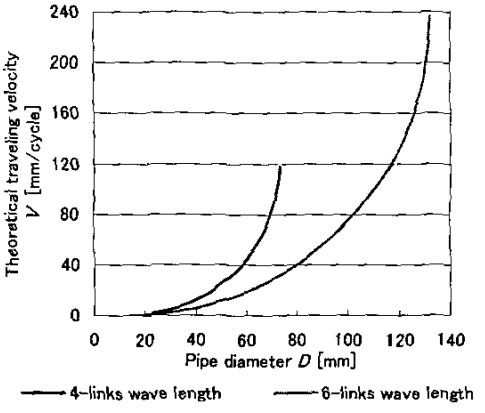

Fig.5 Theoretical traveling velocity

4.Software simulation of the robot traveling

In order to evaluate the moving efficiency of the snaking mechanism, simulation was carried out by using dynamic simulation software (Working Model).

Figure 6 shows an example of the simulation, which shows the robot moving from larger diameter pipe of right side (D mm of width and 1500 mm of length) to smaller diameter pipe of left side (d mm of width and 1500 mm of length). The robot is found to move successfully. Table 1 shows the traveling velocity of this simulation.

Fig.7 shows the simulation of the robot negotiating T-branches. The robot travels from right side to upper side in this simulation. The robot can travel any directions, and this algorism is discussed in detail in section 6.3.

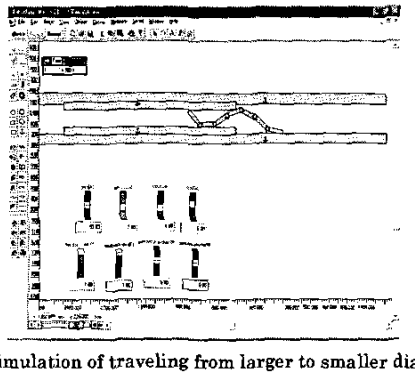

Fig.6 Simulation of traveling from larger to smaller diameter

Table 1 Traveling velocity of the simulation

D [mm] \ d [mm]	70	120	170
120	9.6 [mm/s]	–	–
180	7.7	25.0	–
240	6.6	22.6	44.1

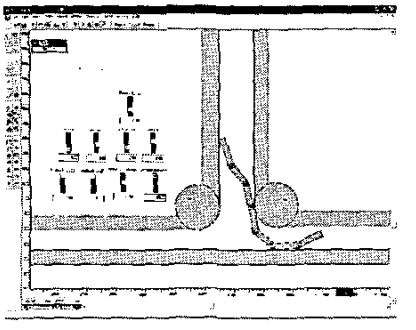

Fig.7 Simulation of negotiating at t-branches

5.Robot design and fundamental experiments

5.1 Configuration of robot

A micro snake-like robot was designed and tested in order to verify the potential of the snaking drive mechanism. The robot consists of 7 links, which are connected serially by 6 rotational joints as shown in Fig.8.

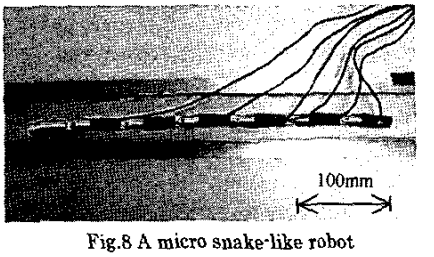

Fig.8 A micro snake-like robot

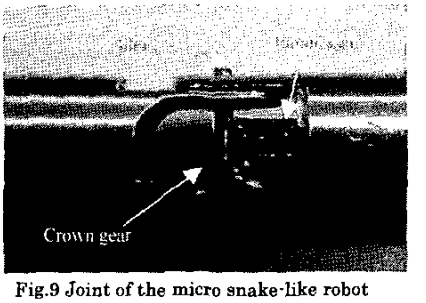

Fig.9 Joint of the micro snake-like robot

Figure 9 shows a joint consisting of a DC electrical motor with reduction gear (reduction rate of 1/64) and an encoder (resolution of 640 pulse/rev), a pinion gear and a crown gear.

Specifications of the elements and dimensions of the robot are shown in Table 2.

Table 2 Specifications of the robot

Robot	ϕ 14×200mm 210g
DC geared motor	Size ϕ 12×47.1mm Output 0.08W Reduction rate 64 : 1 Resolution 640 pulse /rev.
Shaft	ϕ 2×14mm
Pinion gear	Module 0.3 Number of teeth 14
Crown gear	Module 0.3 Number of teeth 30
One link size	ϕ 14×70mm

5.2 Fundamental experiments

To make clear the fundamental traveling properties, fundamental experiments were made by driving the robot between two walls as shown in Fig.10.

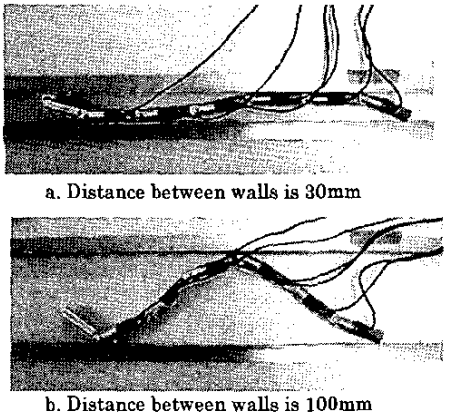

a. Distance between walls is 30mm

b. Distance between walls is 100mm

Fig.10 Fundamental experiment of the robot
(Both a and b are driven by 6-links wave length)

Based on the distance of two walls, the suitable amplitude of the bending angle A and wave length λ are decided by theoretical results in section 3.1.

The experimental results and theoretical results of the robot velocity are shown in Fig.11. The robot could negotiate between two walls whose distance varies from 18 mm to 100 mm with the frequency of 0.2 cycle/sec. And the maximum velocity was 36 mm/s, which was caused by the frequency of 1.0 cycle/sec.

Errors between the experimental results and theoretical results come from the flowing reasons.

Case 1: The experiment results superior to the theoretical results.

At the grip point, the contact force acting between the robot and the walls is sometimes not in the vertical direction of the walls completely. So thrust force occurs to the robot, which drives the robot.

Case 2: The experiment results inferior to the theoretical results.

As the distance between two walls is larger, the joint motor response is delayed more.

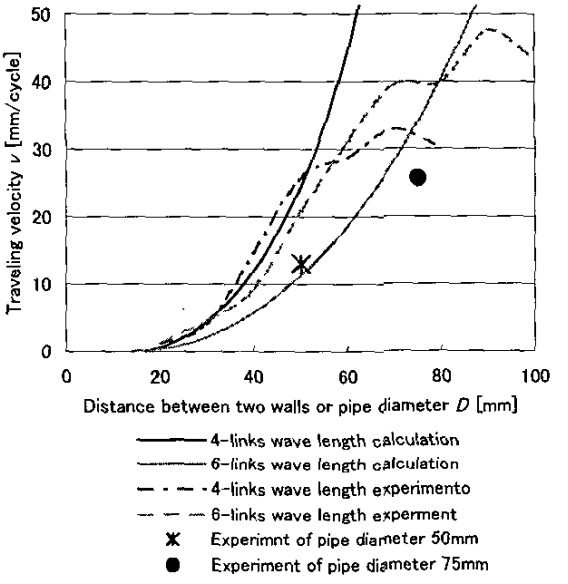

Fig.11 Traveling velocity of the robot

By using pipes made of vinyl chloride, experiments of the robot negotiating pipes were carried out. To increase the grip force between the robot and pipe wall, the robot was improved. Silicone rubber was wound on the part of link covered around the joint, as shown in Fig.12. Two type pipes were used, one is 50 mm in inner diameter, and the other is 75 mm in inner diameter. The traveling velocity of the robot was 4.35 mm/s (13.1 mm/cycle) in the former, 8.55 mm/s (25.7 mm/cycle) in the latter, with the frequency of 0.33 cycle/sec and 6-links wave length.

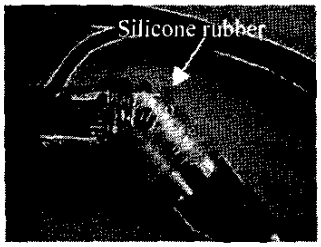

Fig.12 Improvement joint rolled silicon rubber

6.Additional control

6.1 Algorithm of camera image stabilization

To obtain the image of pipe inside, a camera is mounted on the front link. As shown in Fig.13, the front link is necessary to keep its orientation parallel to pipe walls for the stabilization of camera image.

In case of 6-links wave length, the control algorithm is obtained geometrically from Fig.2 and equation (3) as $\theta_2 = -\theta_6$.

Equation (1) leads the bending angles $R(2)$ and $R(6)$ as follows;

$$R(2) = A\sin\left(\omega t - \frac{\pi}{3}\right) \quad , \qquad (7)$$

$$R(6) = A\sin\left(\omega t - \frac{5\pi}{3}\right) \quad . \qquad (8)$$

Then, the bending angle of the 6th joint must be as $R'(6)$ shown below to keep camera orientation parallel to pipe.

$$R'(6) = R(6) + R(2) = A\sin\omega t \quad . \qquad (9)$$

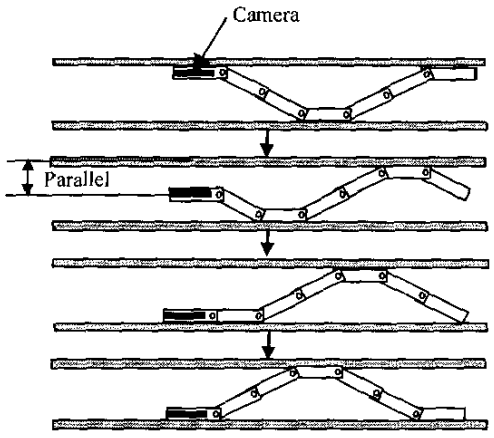

Fig.13 Stabilization control of the camera

6.2 Experiments for the camera image stabilization

Experiments of stabilization of camera image were carried out using the algorism discussed in section 6.1.

Figure 14 shows the experiment of the camera image stabilization. The camera stabilization works well, while some camera image still shakes, which results from backlash of the gears and the friction.

Figure 15 shows the measured angle between the front link to pipe wall in pipe axial direction. In case of applying the camera image stabilization, the value of integration of the angle during one cycle decreased at 45%.

This result was obtained by conditions of 6-liks wave length and frequency of 0.2 cycle/sec.

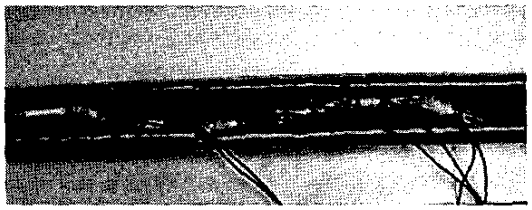
Fig.14 Camera orientation control

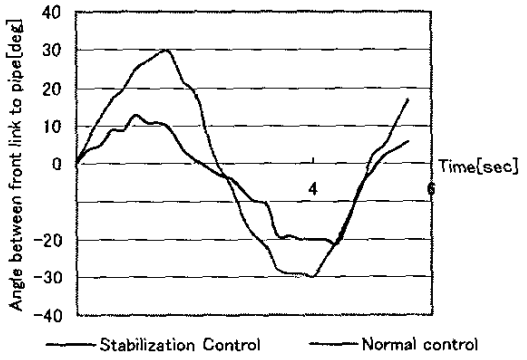

Fig.15 Angle between front link and pipe

6.3 Algorithm of steering at pipe branches

To negotiate pipe branches and elbows, it is effective to add an offset angle to each joint except the front joint. This means adding an offset θ_{ir} to equation(1) as follows.

$$R''(i) = A\sin\left\{\omega t - 2\pi\frac{(i-1)}{\lambda}\right\} + \theta_{ir} \quad , \qquad (10)$$

for i=1, 2, 3, 4, 5 .

The offset leads the thrust direction of the robot.

The front link must be controlled independently to select the paths at pipe branches. This is described as follows;

$$R''(6) = R'(6) + \theta_{6r} = A\sin\omega t + \theta_{6r} \quad . \quad (11)$$

Because the front link is controlled to be kept parallel to pipe, adding the θ_{6r} results in the front link kept in desired angle.

6.4 Experiments of steering at pipe branches

T-branch negotiating experiments were carried out as shown in Fig 16.

The additional control parameters of the joint bending angle, θ_{ir} is controlled manually by an operator handling a joystick and buttons on a control pendant. In this experiment, θ_{1r}~θ_{5r} are set to be equal, θ_{6r} is controlled independently.

The robot can negotiate in any desired direction with manual control.

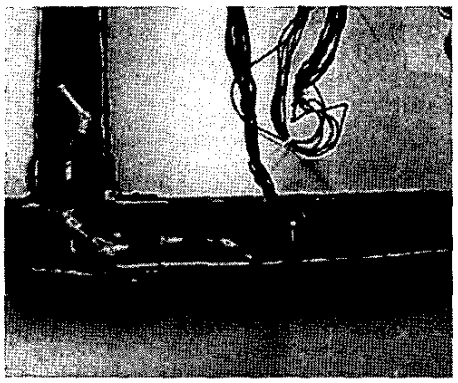

Fig.16 Steering control at T-branch

7.Conclusions

A micro snake-like robot for pipe inspection was developed and tested. The following conclusions can be obtained.

(1) The robot can negotiate space between two walls whose distance varies from 18 mm to 100 mm with maximum velocity is 36 mm/sec.

(2) Shaking of the camera image decreased at 45% by applying control algorithm of the camera image stabilization.

(3) The robot can negotiate T-branches in any desired direction.

Acknowledgment

This work is supported by Electric Technology Research Foundation of Chugoku and also by Japan Institute of Construction Engineering.

References

[1]K.Suzumori et al., "Micro Inspectin Robot for 1-in Pipes", *IEEE/ASME TRANSACTION ON MECHATRONICS*, vol.14, No.3, pp.286-292, 1999.

[2]T.Idogaki et al., "Characteristics of piezoelectric locomotive mechanism for an in-pipe micro inspection machine," *in Proc.IEEE 6th Int. Symp. Micro Machine and Human Sciences*, pp193-198, 1995.

[3]T.Fukuda et al., "Giant magnetostrictive alloy (GMA) applications to micro mobile robot as a micro actuator without power supply cables." *in Proc. IEEE Int. Workshop Micro Electro Mechanical Systems (MEMS)*, pp.210-215, 1991.

[4]M.Nunobiki et al.," An Investigation of Mobility of Inchworm-type robot", *in Proc. France-Japan Congress of Mechatoronics*, pp.113-118, 2002.

[5]M.Mori et al., "Three-dimensional serpentine motion and lateral rolling by Active Cord Mechanism ACM-R3", *in Proc. IROS 2002 (2002 IEEE/RSJ International Conference on Intelligent Robot and Systems)*, pp829-834, 2002,.

[6]K.Suzumori et al., "Flexible Microactuators to Pipeline Inspection Robots", *Transactions of the IMACS/SICE International Symposium on Robotics, Mechatronics and Manufacturing Systems*, pp515-520, 1992.

[7]K.Suzumori et al., "A Miniature Inspection Robot Negotiating Pipes of Widely Varying Diameter", *IEEE International conference on Robotics and Automation*, 2003.